AFRL-SN-HS-TR-2006-001

TERAHERTZ GAIN ON INTERSUBBAND TRANSITIONS IN MULTILAYER DELTA-DOPED p-GaAs STRUCTURES

Robert E. Peale

University of Central Florida
12443 Research Parkway, Ste 207
Orlando FL 32828

5 May 2006

Final Report

AIR FORCE RESEARCH LABORATORY
Sensors Directorate
Electromagnetics Technology Division
80 Scott Drive
Hanscom AFB MA 01731-2909

TECHNICAL REPORT

Title: Terahertz Gain on Intersubband Transitions in Multilayer Delta-Doped p-GaAs Structures

Contract Number: FA871805C0078

Contractor: University of Central Florida

Unlimited, Statement A
Approved for public release; Distribution unlimited.

NOTICE

USING GOVERNMENT DRAWINGS, SPECIFICATIONS, OR OTHER DATA INCLUDED IN THIS DOCUMENT FOR ANY PURPOSE OTHER THAN GOVERNMENT PROCUREMENT DOES NOT IN ANY WAY OBLIGATE THE US GOVERNMENT. THE FACT THAT THE GOVERNMENT FORMULATED OR SUPPLIED THE DRAWINGS, SPECIFICATIONS, OR OTHER DATA DOES NOT LICENSE THE HOLDER OR ANY OTHER PERSON OR CORPORATION; OR CONVEY ANY RIGHTS OR PERMISSION TO MANUFACTURE, USE, OR SELL ANY PATENTED INVENTION THAT MAY RELATE TO THEM.

THIS TECHNICAL REPORT HAS BEEN REVIEWED AND IS APPROVED FOR PUBLICATION.

//signature//

WALTER BUCHWALD
Contract Monitor
Optoelectronics Technology Branch
Electromagnetics Technology Division

//signature//

JOSEPH LORENZO
Chief, Optoelectronics Technology Branch
Electromagnetics Technology Division

//signature//

MICHAEL N. ALEXANDER
Technical Advisor
Electromagnetics Technology Division

REPORT DOCUMENTATION PAGE

Form Approved
OMB No. 0704-0188

1. REPORT DATE *(DD-MM-YYYY)*	**2. REPORT TYPE**	**3. DATES COVERED** *(From - To)*
03-28-2006	Final Report	8/25/2005 to 12/31/2005

4. TITLE AND SUBTITLE
Terahertz Gain on Intersubband Transitions in Multilayer Delta-Doped p-GaAs Structures

5a. CONTRACT NUMBER
FA8718-05-C-0078

5b. GRANT NUMBER

5c. PROGRAM ELEMENT NUMBER
62204F

6. AUTHOR(S)

Robert E. Peale

5d. PROJECT NUMBER
4916

5e. TASK NUMBER
HC

5f. WORK UNIT NUMBER
07

7. PERFORMING ORGANIZATION NAME(S) AND ADDRESS(ES) AND ADDRESS(ES)

University of Central Florida
12443 Research Pkwy, Ste 207
Orlando, FL 32828

8. PERFORMING ORGANIZATION REPORT NUMBER

9. SPONSORING / MONITORING AGENCY NAME(S) AND ADDRESS(ES)

Electromagnetics Technology Division
Sensors Directorate
Air Force Research Laboratory/SNHC
80 Scott Drive
Hanscom AFB, MA 01731-2909

10. SPONSOR/MONITOR'S ACRONYM(S)
AFRL/SNHC

11. SPONSOR/MONITOR'S REPORT NUMBER(S)
AFRL-SN-HS-TR-2006-001

12. DISTRIBUTION / AVAILABILITY STATEMENT
Approved for public release; distribution unlimited

13. SUPPLEMENTARY NOTES
Public Release Clearance: ESC 06-0552, dtd 5 May 2006

14. ABSTRACT

Report developed under contract for FA8718-05-0C-0078. The purpose of the research was to theoretically test a concept for a terahertz laser that might be grown from GaAs using vapor-phase-epitaxial growth facilities at AFRL/SNHC Hanscom AFB. Monte Carlo simulation of hole transport in multilayer delta-doped p-GaAs/GaAs structures with crossed electric and magnetic fields applied were performed to investigate possibilities of the terahertz amplification by vertical inter-valence-band light-to-heavy hole transitions. The results are compared to those calculated for uniformly doped bulk p-GaAs and recently proposed p-Ge/Ge structures. The improvement in the gain for delta-doped p-GaAs structures is about ~ 2 – 3 times over bulk p-GaAs. Terahertz laser generation in the proposed GaAs structure appears feasible. Potential applications for the considered laser device include sensing of chem/bio agents and explosives, biomedical imaging, non-destructive testing, and communications.

15. SUBJECT TERMS
Terahertz, far-infrared, laser, GaAs, Monte-Carlo

16. SECURITY CLASSIFICATION OF:			**17. LIMITATION OF ABSTRACT**	**18. NUMBER OF PAGES**	**19a. NAME OF RESPONSIBLE PERSON**
					Walter Buchwald
a. REPORT	**b. ABSTRACT**	**c. THIS PAGE**	SAR	24	**19b. TELEPHONE NUMBER** *(include area code)*
Unclassified	Unclassified	Unclassified			

Standard Form 298 (Rev. 8-98)
Prescribed by ANSI Std. 239.18

TABLE OF CONTENTS

LIST OF FIGURES

1.0 Introduction

GaAs is a potential active medium for inter-valence-band (IVB) hot-hole THz lasers [1-3]. Monte Carlo simulations have shown that bulk uniformily-doped GaAs should have acceptable performance [4]. However, due to doubled (see below) impurity scattering rate (a consequence of lower dielectric constant) in GaAs relative to Ge, THz gain in p-GaAs devices is expected to be lower than in the well-established p-Ge lasers. Compared with Ge, GaAs has additional factors of polar optical phonon and acoustic piezoelectric phonon scattering processes. The latter is usually unimportant, but the polar optical phonon scattering has a significant role. Monte Carlo simulation results for GaAs illustrate these features.

For the IVB mechanism, the inverted population grows at certain ratios of applied, crossed, electric- and magnetic-fields, when light holes are accumulated on closed trajectories below the optical phonon energy, while heavy holes undergo rapid optical phonon scattering. Fig. 1 is a schematic quasiclassical explanation of the IVB laser mechanism that is valid at low applied fields where Landau-level spacing is much less than carrier kinetic energy. The emission of polar (circle) and non-polar (starburst) optical phonons is indicated. Polar optical-phonon scattering in III-V compounds [5] provides a “hard roof” for hot holes. Most of the scattering events occur right beyond the optical phonon threshold, which is 0.035 meV [6] for GaAs. In contrast, in non-polar semiconductors (Ge, Si) the optical-phonon emission rate grows slowly with energy from the threshold value. Light-hole life time, which is responsible for the inversion population and for the gain, is determined by acoustic phonon scattering, ionized impurity scattering, and carrier-carrier interaction. This limits operation of IVB hot-hole laser, which has been experimentally realized only for p-Ge, to low temperatures ($T < 20$ K) and low carrier concentration ($p \sim 10^{14}$ cm^{-3}) [1-3]. The IVB amplification mechanism illustrated in Fig. 1 provides wide tunability of p-type hot-hole devices in the terahertz frequency range (1.5 – 4.2 THz for p-Ge).

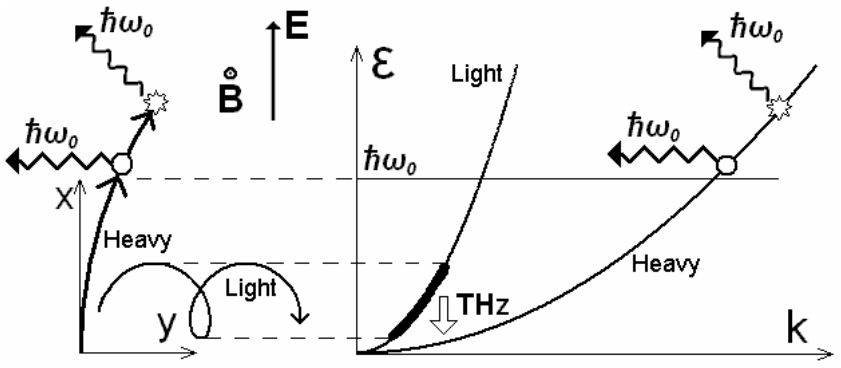

Figure 1 Schematic of quasi-classical explanation for intersubband hot-hole laser.

We recently developed a terahertz laser concept based on inter-subband transitions of holes with transport in crossed electric E and magnetic B fields in a planar periodically doped p-Ge/Ge structure [7-10]. The design, shown schematically in Fig. 2, achieves spatial separation of hole accumulation regions from the doped layers, which reduces ionized-impurity scattering and carrier-carrier scattering for the majority of light holes, allowing significant increase of total carrier concentration without affecting light hole life time. The resulting increase in gain over the bulk p-Ge laser promises to raise maximum operation temperatures to 77 K. At the same time the proposed laser retains the intersubband mechanism with its wide tuning range 1-4 THz. Moreover, this crystalline-Ge device can be grown by chemical vapor deposition (CVD), which allows active thicknesses comparable to the THz wavelength, thus allowing low-loss quasi-optical cavity solutions. As soon as we have developed a THz laser concept based on CVD epitaxial Ge devices, it becomes very interesting to consider the possibility of realizing a similar structure based on GaAs, because of the highly sophisticated technology available for epitaxial growth of this material.

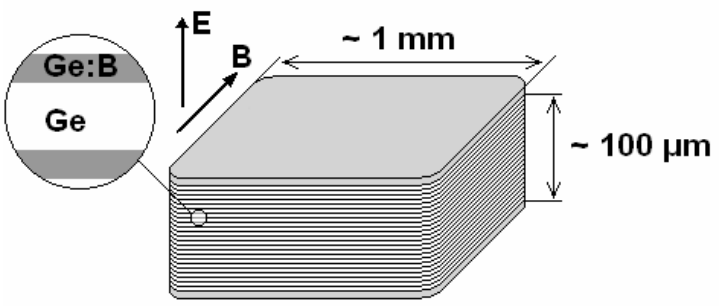

Figure 2 Homoepitaxial multilayer p-type semiconductor structure THz laser concept for germanium. The layer period is chosen to be 200 –500 nm, which is larger than the light hole cyclotron orbit, but smaller than that for heavy holes. The doped layers are ~10% as thick as the period. Light holes are shown by Monte Carlo simulation to accumulate in the undoped layers where their life time is enhanced by reduced impurity scattering. This scheme allows much higher average carrier concentrations than for uniformily doped bulk, giving a corresponding increase in gain. The stack thickness achievable for germanium by chemical vapor deposition is estimated to be 100 μm. In the case of a GaAs structure, the total stack thickness that can been achieved by vapor phase epitaxy would be up to 800 microns, giving a low-loss quasioptical cavity solution.

2.0 Methods

Hole dynamics, hole distribution functions, and the gain on direct optical light-to-heavy hole transitions in p-GaAs are calculated by the Monte-Carlo simulation method using classical motion equations and hole scattering probabilities [11,12]. Two valence subbands (light and heavy holes) with isotropic and parabolic dispersion laws are considered. The isotropic approach is justified by the relatively small warping of the GaAs valence band. We can neglect quantum confinement effects because the considered structure has no heteroboundaries, only delta-doped layers. We also neglect Landau quantization, which is a good approximation for magnetic fields of 3 – 4 T and below. Time or ensemble averaged momentum and position yield the hole distribution functions $f_{l,h}(\mathbf{k},\mathbf{r})$ (subband (l,h), wavevector **k**, and coordinate **r**). The distribution functions were considered uniform in the horizontal planes according to the geometry of the problem. The standard Rees rejection technique chooses among scattering processes [11]. The rate of each scattering process is given by a temperature-dependent analytic expression. Polar and non-polar optical phonon scattering is treated in a deformation potential approximation [5]. Acoustic phonon scattering is simplified according to [13]. Inelasticity for acoustic phonon scattering is included [14].

Piezoelectric scattering is treated according to [15]. Brooks-Herring model [15] with inverse Debye screening length and Yukawa potential was used for ionized impurity scattering. Hole-hole scattering was calculated according to [16]. Iteration determines the self-consistent solution of the Poisson equation and thereof the spatial carrier distribution and potential profile. The small signal gain is calculated as the difference between the gain on direct intersubband (light to heavy hole) transitions and free carrier absorption assisted by phonons and ionized impurities [17,18]. Up to liquid nitrogen temperatures and impurity concentrations of ~ 10^{15} - 10^{16} cm^{-3}, the main contribution to free carrier absorption in GaAs comes from polar optical phonon emission by heavy holes. Lattice absorption [19] was not included in the calculations.

Strong intersubband (heavy-to-light) polar-optical phonon scattering in p-GaAs populates the light-hole subband. In contrast to non-polar optical phonon scattering, most of these scattering events occur right beyond the sharp energy threshold for polar-phonon scattering (see Fig. 1). As a result, after emission of an optical phonon light holes are created with very small kinetic energy. These slow holes experience very strong ionized impurity and hole-hole scattering, which is enhanced in GaAs compared to Ge because of the smaller relative permittivity (ε_r = 12.9 for GaAs vs 16.0 for Ge). These holes are quickly accelerated by the applied electric field, but they return to the low-energy range on each loop of cyclotron trajectory in crossed fields. The ionized impurity scattering is the dominant light-subband-depopulating mechanism. Similarly, ionized impurity scattering of heavy holes is also stronger in GaAs compared to Ge. Acoustic deformation potential scattering rates in GaAs are similar to rates in Ge. Piezoelectric scattering is weak and can be neglected. In order to maintain inverted distribution of holes and to reduce the effect of ionized impurity scattering for light holes in GaAs, the magnitude of the applied fields must be higher than typical for the p-Ge laser (E = 1 – 2 kV/cm, B = 1 – 2 T).

3.0 Calculations for Uniformly Doped Materials

For direct comparison of the scattering effects in germanium and GaAs, the distribution functions averaged over directions are plotted in Fig. 3 for both materials in strong crossed electric (E = 4 kV/cm) and magnetic (B = 3 T) fields at T = 20 K for carrier concentration p = 2.5 x 10^{14} cm^{-3}.

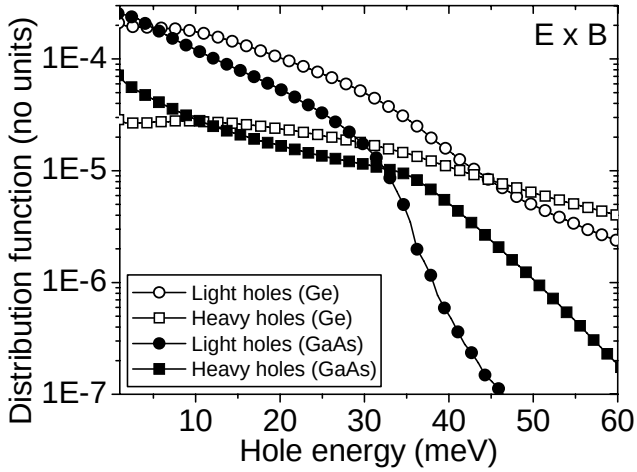

Figure 3 Calculated distribution functions of light and heavy holes in Ge and GaAs. E = 4 kV/cm, B = 3 T, T = 20 K, and p = 2.5x10^{14} cm^{-3}.

The hole distribution for GaAs is shifted into the low-energy region by the sharp threshold in polar optical phonon scattering described above. Direct LH transition amplification and free-carrier absorption calculated for bulk p-Ge and p-GaAs are presented in Figs. 4 and 5. The simulation parameters for Ge (GaAs) are E = 1.5 kV/cm, B = 1.2 T, T = 10K, p = 10^{14} cm^{-3} (E = 4 kV/cm, B = 3.5 T, T = 10K, p = 2 x 10^{14} cm^{-3}).

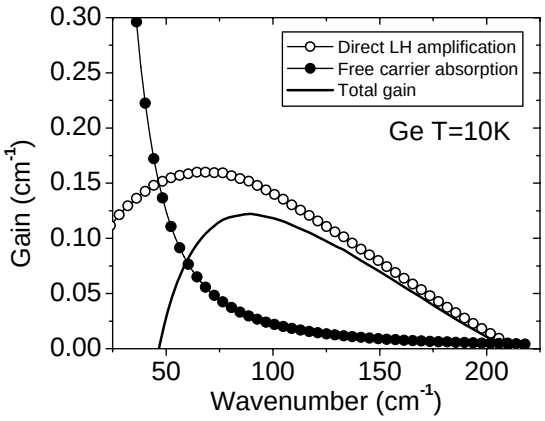

Figure 4 Calculated inter-valence-band gain and free carrier absorption in bulk p-Ge with carrier concentration 10^{14} cm^{-3}. E = 1.5 kV/cm, B = 1.2 T, T = 10K. Total gain (smooth curve) is the difference between two curves with symbols.

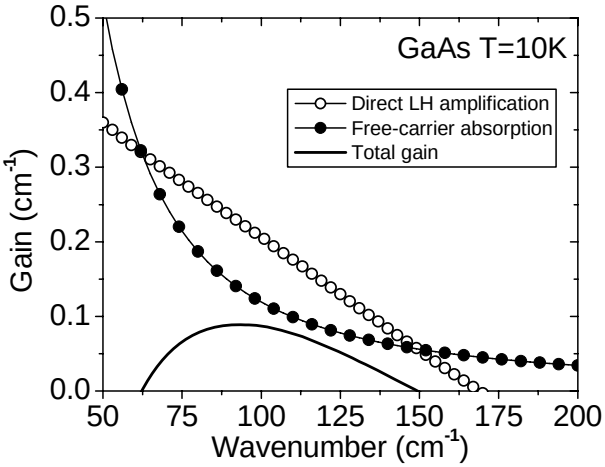

Figure 5 Calculated inter-valence-band gain and free carrier absorption in bulk p-GaAs with carrier concentration $2x10^{14}$ cm^{-3}. E = 4 kV/cm, B = 3.5 T, and T = 10K. The total gain (smooth curve) is the difference between two curves with symbols.

The total gain is smaller for GaAs than for Ge, despite the much higher applied fields and twice higher hole concentration. Fields need to be increased over those for Ge, in principle, to achieve *any* positive gain in GaAs. One reasons for this is the almost twice smaller oscillator strength for GaAs [20]. A second reason is stronger free carrier absorption, which arises because phonon scattering rates are higher and because the inversion between light and heavy hole subbands is shifted to a low energy range (see

Fig. 3). Compared with Ge, direct inter-valence-band amplification in GaAs reaches a maximum at lower wavenumbers, as suggested by the distribution functions Fig. 3.

The maximum value of the gain is plotted as a set of contours in Fig. 6 as a function of the applied fields. The interval between contour plots is 0.025 cm^{-1}. Here and below, the contours are spline-interpolated. The waves in the contours are caused by the interpolation to the limited set of data points, which occur at every grid intersection.

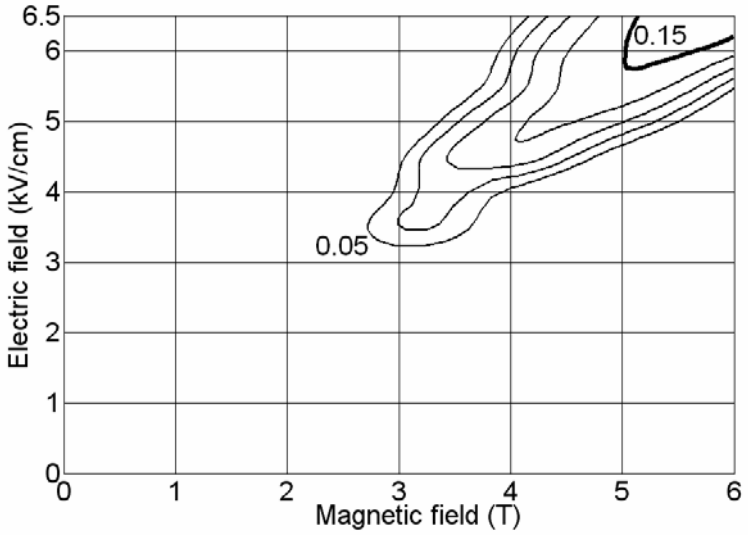

Figure 6 Gain for uniformly doped p-GaAs as a function of applied fields. Simulation parameters are $p = 2x10^{14}$ cm^{-3}, T = 10 K.

As has been shown previously [4], the optimal ratio of fields and their magnitudes must be different for the two materials, and the gain in GaAs can be increased by applying higher electric (~ 8 kV/cm) and magnetic (~ 7 T) fields. However, the validity of classical approach for Monte Carlo simulation under these extreme conditions becomes questionable. Performance of p-GaAs hot-hole lasers would be improved by the periodic doping scheme, suggested in the introduction, by which impurity scattering is eliminated from the active region. The same device concept with vertical transport, which has been demonstrated theoretically for Ge[7], can be applied directly to GaAs.

4.0 Calculations for Delta Doped Structure

Delta doped p-GaAs/GaAs structure with doping period *d* = 200 nm (20% doped, 80% undoped), and average carrier concentration $2x10^{14}$ cm^{-3} has been used for preliminary gain estimations. The electric and magnetic fields are 4 kV/cm and 3.5 T, respectively, and the lattice temperature is 10 K. Calculated spatial distribution of light and heavy holes across two structure periods is shown in Fig. 7.

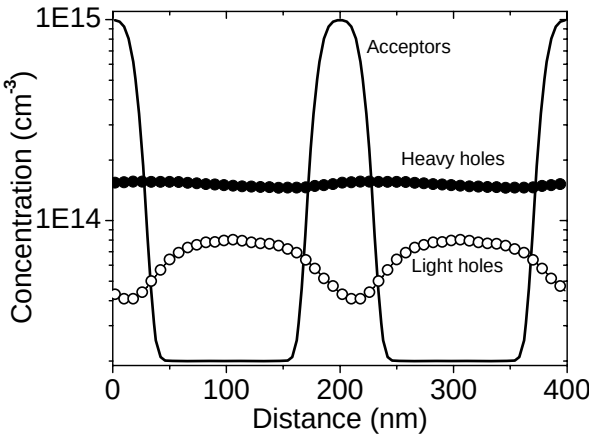

Figure 7 Distribution of light and heavy hole concentrations across the structure. Most of the light holes are concentrated in the undoped region between two doped layers. E = 4 kV/cm, B = 3.5 T, *d* = 200 nm, *p* = $2x10^{14}$ cm^{-3}.

The resulting spatial-spectral gain distribution is shown in Fig. 8. Strong inversion is observed in the regions of undoped GaAs. The doped layers are absorbing.

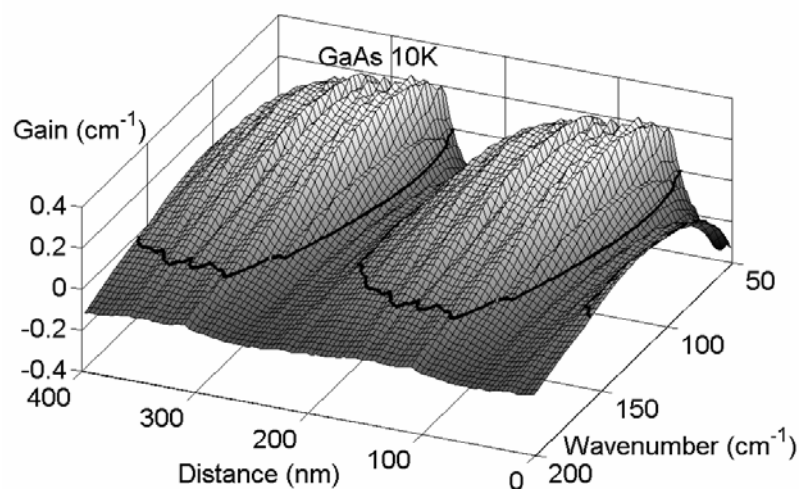

Figure 8 Spatial-spectral gain distribution across two structure periods (N_{av} = 2 x 10^{14} cm^{-3}, *d* = 200 nm, E = 4 kV/cm, B = 3.5 T, T = 10 K) with free carrier absorption included.

The spatially averaged net gain in the structure is presented in Fig. 9. Compared to Fig. 5 for bulk p-GaAs the gain is approximately twice higher. The gain spectrum is ~ 50 – 150 cm^{-1} wide, but this will be modified by the lattice absorption (not include in the calculations). Note that all simulation parameters are the same as in Fig. 5 for bulk GaAs (fields, average concentration, temperature) except the doping profile, so that the observed improvement is a purely effect of the selective doping. As will be shown below, an additional improvement of the gain by increase in the carrier concentration, as was observed for p-Ge/Ge structures [7-10], is not achievable for GaAs.

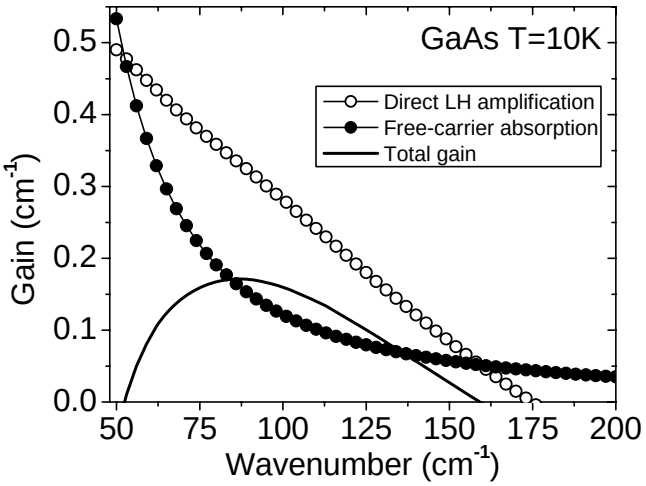

Figure 9 Calculated spatially averaged terahertz gain α in the structure with parameters as for Fig. 5. The total gain (smooth curve) is the difference between two curves with symbols.

Next, we optimize the structure by varying the simulation parameters to maximize the gain. The gain dependence on the magnitude of the applied fields for the structure with fixed doping parameters (p = 2x10^{14} cm^{-3}, d = 250 nm, 10% doped, 90% undoped) is shown in Fig. 10. The interval in the gain between the contour plots is 0.025 cm^{-1}.

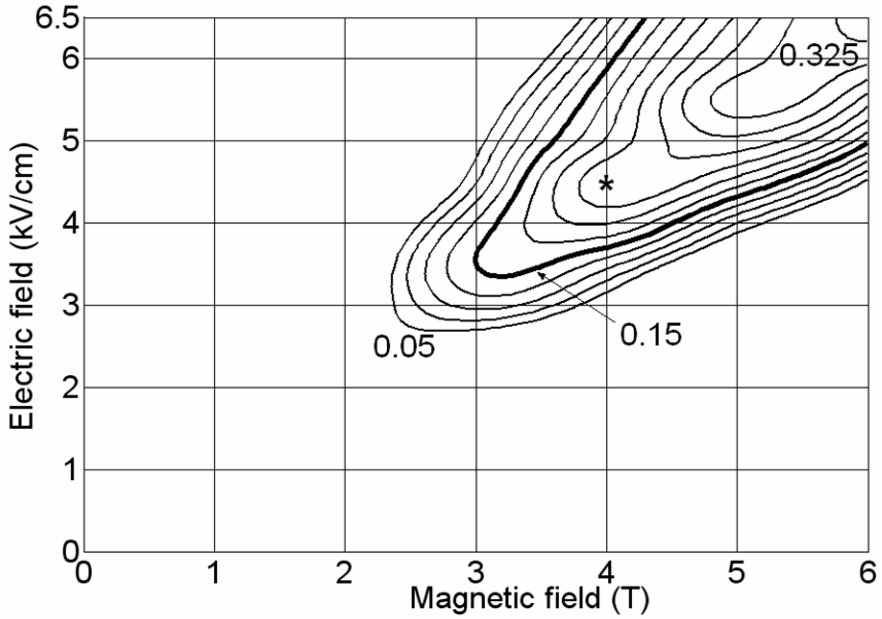

Figure 10 Gain for delta-doped p-GaAs/GaAs structure as a function of applied fields. Simulation parameters are p = 2x10^{14} cm^{-3}, d = 250 nm (10% doped, 90% undoped), T = 10 K.

Comparison of Figs. 6 and 10 shows that the acceptable range of the applied fields is wider for delta doped structure than for the uniformly doped GaAs (see 0.15 cm^{-1} contours in both figures). The gain achievable for delta doped structure is about twice higher than for bulk p-GaAs.

Next, we vary the doping parameters (structure period and average carrier concentration) while holding the applied fields fixed. These fields (E = 4.5 kV/cm, B = 4 T) correspond to the star in Fig. 10). The relative thickness of the p-GaAs doped layers is fixed and equal to 10% of the period as before. The gain surface is shown in Fig. 11 by the contour plots with 0.025 cm^{-1} intervals.

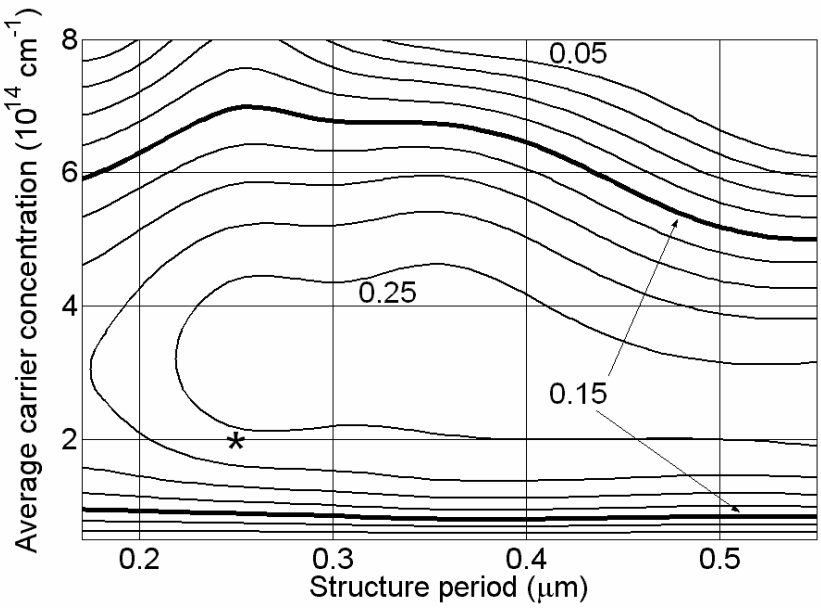

Figure 11 Gain for p-GaAs/GaAs structure as a function of carrier concentration and structure period. Simulation parameters E = 4.5 kV/cm, B = 4T, T = 10 K. The relative thickness of the doped p-GaAs layers is 10% of the structure period.

In contrast to p-Ge/Ge structures [7-10], the optimal average carrier concentration for the delta doped p-GaAs/GaAs structure is comparable to that for uniformly doped p-

GaAs [4] and equal to ~ $2x10^{14}$ – $4x10^{14}$ cm^{-3}. The optimal range of the structure period is 250 – 500 nm for the chosen fields. As can be seen from the Fig. 11, the gain is very sensitive to the structure period at high doping concentrations. This is caused by the distortion of electric potential across the structure period, which changes the ratio of the local electric and magnetic fields and hole lifetime. At low carrier concentration the gain surface does not show such a strong dependence as soon as the average light hole cyclotron orbit (which decreases with increase in magnetic fields) fits inside the undoped layer (see decrease in the gain in the low period part of the Fig. 11) to provide a long lifetime of the light hole and therefore inversion.

References

1. E. Bründermann, “Widely Tunable Far-Infrared Hot-Hole Semiconductor Lasers” in *Long wavelength infrared semiconductor lasers*, edited by H. K. Choi (Wiley, NJ, 2004), pp. 279-343.

2. V. N. Shastin, “Hot hole inter-sub-band transition p-Ge FIR laser”, Opt. Quantum Electron. **23**, S111 (1991).

3. A. A. Andronov, A. M. Belyantsev, E. P. Dodin, V. I. Gavrilenko, Yu. L. Ivanov, V. A. Kozlov, Z. A. Krasil'nik, L. S. Mazov, A. V. Muravjov, I. M. Nefedov, V. V. Nikanorov, Yu. N. Nozdrin, S. A. Pavlov, V. N. Shastin, V. A. Valov, and Yu. B. Vasil'ev, “Tunable hot hole FIR lasers and CR masers”, *Physica B* **134**, 210 (1985).

4. P. Kinsler and W. Th. Wenckebach, “Hot-hole lasers in III-V semiconductors”, *J. Appl. Phys.* **90**, 1692 (2001).

5. T. Brudevoll, T. A. Fjeldly, J. Baek, and M. S. Shur, “Scattering rates for holes near the valence-band edge in semiconductors,” *J. Appl. Phys.* **67**, 7373 (1990).

6. M. Neuberger**, *Handbook of Electronic Materials***, vol. 2 (Plenum, New York 1971).

7. M. V. Dolguikh, A.V. Muravjov, R. E. Peale, M. Klimov, O. A. Kuznetsov, E. A. Uskova, “Terahertz gain on intersubband transitions in multilayer delta-doped p-Ge structures,” *J. Appl. Phys.* **98**, 023107 (2005).

8. M. V. Dolguikh, A. V. Muravjov, R. E. Peale, “Intervalence band THz laser in selectively-doped semiconductor structure,” in *Novel In-Plane Semiconductor Lasers III* edited by C. F. Gmachl and D. P. Bour, Proc. SPIE **5365**, 184 (2004).

9. M. V. Dolguikh, A. V. Muravjov, and R. E. Peale, “Selectively doped germanium THz laser,” in *Terahertz for Military and Security Applications*, edited by R. J. Hwu and D. L. Woolard, Proc. SPIE **5411**, 207 (2004).

10. M. V. Dolguikh, A. V. Muravjov, and R. E. Peale, “Gain comparison for periodically delta-doped p-Ge structures with vertical and in-plane transport,” in *Terahertz for Military and Security Applications*, edited by R. J. Hwu, D. L. Woolard, M. J. Rosker, Proc. SPIE **5790**, 161 (2005).

11. C. Jacoboni and L. Reggiani, “The Monte Carlo method for the solution of charge transport in semiconductors with applications of covalent materials,” *Rev. Mod. Phys.* **55**, 645 (1983)

12. C. Jacoboni, R. Brunetti and P. Bordone, “Monte Carlo simulation of semiconductor transport,” in *Theory of Transport Properties of Semiconductor Nanostructures*, ed. Eckehard Scholl, (Chapman & Hall, London, 1998), p. 59.

13. J. D. Wiley, “Polar mobility of holes in II-V compounds,” *Phys. Rev. B* **4**, 2485 (1970).

14. E. V. Starikov, P. N. Shiktorov, “Numerical simulation of far infrared emission under population inversion of hot sub-bands”*, Optical and Quantum Electronics*, **23**, S177, (1991).

15. B. K. Ridley, *Quantum Processes in Semiconductors* (Oxford, NY, 1999).

16. M. V. Dolguikh, A. V. Muravjov, and R. E. Peale, “Intervalenceband hole-hole scattering in cubic semiconductors”, Phys. Rev. B, in press (2006).

17. Yu. K. Pozhela, E. V. Starikov, and P. N. Shiktorov, “Far infrared absorption by hot holes in p-Ge under E⊥B fields,” *Phys. Stat. Sol. (b)* **128**, 653 (1985).

18. M. V. Dolguikh, “Monte Carlo simulation of hole transport and terahertz amplification in multilayer delta doped semiconductor structures”, *PhD thesis*, University of Central Florida (2005).

19. R. Brazis and F. Keilmann, “Lattice absorption of Ge in the far infrared,” *Solid State Comm.* **70**, 1109 (1989).

20. M. V. Dolguikh, A.V. Muravjov, R. E. Peale, R. A. Soref, D. Bliss, C. Lynch, and D. W. Weyburne, “Toward hot-hole THz lasers in homoepitaxial Si and GaAs with layered doping,” in *Nanoengineering: Fabrication, Properties, Optics, and Devices II,* Proc. SPIE **5931**, 310 (2005).